Opposite pressure effects in the orbitally-induced Peierls phase transition systems $CuIr_2S_4$ and $MgTi_2O_4$

Long Ma,[1] Hui Han,[1,2] Wei Liu,[1,2] Kaishuai Yang,[3] Yuanyuan Zhu,[4] Changjin Zhang,[1] Li Pi,[1,5] Dayong Liu,[3,*] Lei Zhang,[1,†] and Yuheng Zhang[1,5]

[1]*High Magnetic Field Laboratory, Chinese Academy of Sciences, Hefei 230031, China*

[2]*University of Science and Technology of China, Hefei 230026, China*

[3]*Key Laboratory of Materials Physics, Institute of Solid State Physics, Chinese Academy of Sciences, Hefei 230031, China*

[4]*School of Arts and Sciences, Shanxi University of Science and Technology, Xi'an 710021, China*

[5]*Hefei National Laboratory for Physical Sciences at the Microscale, University of Science and Technology of China, Hefei 230026, China*

(Dated: January 23, 2017)

Abstract

The iso-spinel structural systems $CuIr_2S_4$ and $MgTi_2O_4$ exhibit phase transitions of the similar nature at $\sim$ 230 K and $\sim$ 260 K respectively, which are explained as an orbitally-induced Peierls phase transition. However, in this work, we uncover that applied pressure has opposite pressure effects on the phase transitions in $CuIr_2S_4$ and $MgTi_2O_4$. As pressure increases, the phase transition temperature (T_{MI}) for $CuIr_2S_4$ increases while that for $MgTi_2O_4$ decreases. In addition, the phase transition intensity becomes weaker for $CuIr_2S_4$ but gets stronger for $MgTi_2O_4$ under pressure. Our results indicate that the applied pressure suppresses the metallic phase in $CuIr_2S_4$, while enhances that in $MgTi_2O_4$. Combining the experimental observations with first-principle electronic structure calculations, we suggest that the opposite pressure effects in $CuIr_2S_4$ and $MgTi_2O_4$ originate from the different orbital ordering configurations (d_{xy}, d_{yz}/d_{xz}) caused by different lattice distortions in these two systems. Our findings directly indicate that the interplay between the orbital and lattice degrees of freedom plays an important role in the orbitally-induced Peierls phase transition.

PACS numbers: 71.30.+h, 71.45.Lr, 72.80.Ga

Keywords: orbitally-induced Peierls instability, pressure effect, metal-insulator phase transition

*Corresponding author. Email: dyliu@theory.issp.ac.cn

†Corresponding author. Email: zhanglei@hmfl.ac.cn

I. INTRODUCTION

The interplay between charge, orbital, spin, and lattice degrees of freedom results in complicated physical phenomena, among which the orbitally-driven dimensionality transformation in a three-dimensional network is very rare [1–5]. The prominent example is known as an orbitally-induced Peierls phase transition, which has been discovered in the iso-spinel structural materials $CuIr_2S_4$ and $MgTi_2O_4$ [6]. At room temperature, both systems have cubic unit cells belonging to space group $Fd\bar{3}m$. Upon temperature decreasing, $CuIr_2S_4$ exhibits a first order metal-insulator transition at $\sim$ 230 K, which is accompanied by a sharp decline of magnetism caused by spin-dimerization and emergence of an octamer ordering in the low temperature pseudo-tetragonal (strictly monoclinic) phase [7–10]. Similarly, $MgTi_2O_4$ undergoes a metal-insulator transition at $\sim$ 260 K, which is characteristic of a sharp reduction of magnetism and appearance of a helical ordering in the low temperature tetragonal phase [11–13]. Both systems form a spin singlet state in the low temperature phases [14–17].

D. I. Khomskii and T. Mizokawa proposed to explain these phase transitions as an orbitally-induced Peierls phase transition, where the anisotropic coupling of orbitals caused by the partially filled t_{2g} band along a certain direction gives rise to the orbitally-induced Peierls instability [18]. For $CuIr_2S_4$, the $5d$ level of Ir ion is split by the crystal filed of IrS_6 octahedron into doublet e_g level with higher energy and triplet t_{2g} level with lower energy. Due to the band-Jahn-Teller effect, the coupling of $5d_{xy}$ orbitals of Ir^{4+} ions along the xy direction leads to the dimerization of Ir^{4+}-Ir^{4+} bonds along the [110] direction [19]. For $MgTi_2O_4$, the $3d$ level of Ti ion is split by the crystal filed of TiO_6 octahedron and band-Jahn-Teller effect. However, because of one electron per Ti^{3+} ion, the still degenerate $3d_{xz}$ and $3d_{yz}$ levels are alternatively occupied. The coupling of alternative $3d_{xz}$ and $3d_{yz}$ orbitals of Ti^{3+} results in helical dimers with compressive Ti-Ti distances alternating with long bonds along the [001] direction [13].

It has been demonstrated that these orbitally-induced phase transitions are sensitive to the hydrostatic pressure P [20, 21]. The transition temperature in $CuIr_2S_4$ increases as the pressure gets higher [22]. However, the pressure effect in $MgTi_2O_4$ has not been reported so far. In this work, through the modulation of lattice structures by hydrostatic pressure, we find that the orbitally-induced Peierls phase transitions in $CuIr_2S_4$ and $MgTi_2O_4$ have

opposite behaviors under pressure. The transition temperature of $CuIr_2S_4$ shifts toward higher values as the pressure increases, while that of $MgTi_2O_4$ toward lower values. Moreover, the transport behavior becomes more insulating as the pressure increases in $CuIr_2S_4$, while it shows a metallic tendency in $MgTi_2O_4$. Combining the experimental observations with first-principle calculations, we propose that the opposite pressure effects in $CuIr_2S_4$ and $MgTi_2O_4$ originate from different one-dimensional band-Jahn-Teller effects in these two systems.

II. EXPERIMENT

A polycrystalline sample of $CuIr_2S_4$ was prepared by the solid-state reaction method, and a polycrystalline sample of $MgTi_2O_4$ was synthesized using the spark plasma sintering (SPS) method. All the sample preparation procedures were carried out in argon atmosphere. The preparation methods and the physical properties have been reported in details elsewhere [23, 24]. The resistivity measurements were performed using the conventional four-probe method with the temperature varied using a closed He-gas cycle refrigerator. For the hydrostatic high-pressure resistivity measurements, we used a clamp-type piston pressure cell and employed Daphne 7373 oil as the medium to transmit pressure with a high level of high homogeneity. To calibrate the pressures at room temperature, we used Cu_2O powder as a manometer, whose nuclear quadrupole resonance frequency as a function of pressure has been determined very accurately [25]. The numerical calculations were performed by the full potential linearized augmented-plane-wave (FP-LAPW) scheme based on density functional theory (DFT) in the WIEN2K package [26].

III. RESULTS AND DISCUSSION

Figures 1 (a) and (b) show the temperature dependence of resistivity [$\rho(T)$] for $CuIr_2S_4$ and $MgTi_2O_4$ under different pressures. Under ambient pressure, $CuIr_2S_4$ exhibits a typical metal-insulator phase transition with temperature decreasing, as given in Fig. 1 (a). The value of resistivity undergoes a change of about three orders of magnitude at $\sim$ 230 K from metallic state to insulating phase. The thermal hysteresis during cooling and heating indicates a first-order phase transition. As the pressure increases, the phase transition

moves toward higher temperature direction, and the hysteresis area shrinks. This pressure induced tendency is consistent with the magnetization measurement [27] and other report [22]. Similarly, as the temperature decreases under ambient pressure, $MgTi_2O_4$ displays a transition from metallic state to insulating phase with a change of two orders of magnitude in $\rho(T)$ at $\sim$ 260 K, as shown in Fig. 1 (b). The transition is also of first order as signified by a thermal hysteresis curve of $\rho(T)$. The high temperature phase in $MgTi_2O_4$ is still controversial. Zhou *et al*. suggested that $MgTi_2O_4$ is a semiconductor above the transition temperature. However, this explanation is inconsistent with the Pauli paramagnetism in higher temperature regime [12]. Isobe *et al*. proposed that the high temperature phase is a metallic state, where the slow increase of ρ upon temperature decreasing is due to the grain boundary resistance [11]. In this paper, we roughly treat the first-order phase transitions in both systems as metal-insulator transitions, and define transition temperature as T_{MI} uniformly. In contrast to $CuIr_2S_4$, Fig. 1 (b) shows that T_{MI} for $MgTi_2O_4$ shifts to lower temperature direction and the hysteresis area expands when the applied pressure increases.

To better understand the pressure effects on the phase transitions, Figs. 1 (c) and (d) present the temperature dependence of differential resistivity $[d\rho/dT(T)]$ under different pressures for $CuIr_2S_4$ and $MgTi_2O_4$, respectively. There is a peak in each $d\rho/dT(T)$ curve, which is caused by the change of resistivity at T_{MI}. The height of the peak quantifies the intensity of the phase transition [22]. For $CuIr_2S_4$ in Fig. 1 (c), the peak moves toward higher temperature direction and its height becomes smaller as the pressure increases. The reduction of the height suggests that the intensity of the phase transition is weakened by the pressure. For $MgTi_2O_4$ in Fig. 1 (d), the peak shifts to lower temperature direction and its height gets larger as the pressure increases. The increase of the height implies that the phase transition is enhanced by the pressure.

The transition temperature T_{MI} can be actually determined by the peak in $d\rho/dT(T)$ curve. Figures 2 (a) and (b) plot T_{MI} as a function of pressure for $CuIr_2S_4$ and $MgTi_2O_4$, respectively. One can see that T_{MI} for $CuIr_2S_4$ increases almost linearly with the applied pressure. The linear fitting of T_{MI} as a function of pressure has been performed using both the heating and cooling curves, where the value extracted from the heating (cooling) curve is denoted as T^H_{MI} (T^C_{MI}). For $CuIr_2S_4$, T^H_{MI} increased with pressure at a speed of 21.32 K/GPa, while T^C_{MI} increases at 22.49 K/GPa. These results are consistent with previously reported values [22, 27]. For $MgTi_2O_4$, T_{MI} decreases linearly with the applied pressure, where T^H_{MI}

decreases at a speed of 6.14 K/GPa and T_{MI}^{C} decreases at 6.20 K/GPa. Meanwhile, the width of the phase transition (ΔT), which is defined as the peak-to-peak width in the $d\rho/dT(T)$ curves as illustrated in the inset of Fig. 1 (c), also qualifies the change of the phase transition with pressure. The pressure dependence of ΔT for $CuIr_2S_4$ and $MgTi_2O_4$ are given in Figs. 2 (c) and (d) respectively (the lines are guided on eye). As the pressure increases, ΔT decreases in $CuIr_2S_4$ while it increases in $MgTi_2O_4$, which corresponds to the shrinkage and expansion of the thermal hysteresis in $CuIr_2S_4$ and $MgTi_2O_4$ respectively. The shrinkage and expansion of the phase transitions also indicate that the phase transition is weakened in $CuIr_2S_4$ while it is enhanced in $MgTi_2O_4$ as the pressure increases.

The opposite pressure effects can also be understood by examining how the metallic phases change as quantified by the resistivity values, *i.e.* suppression and expansion of the metallic phase. Figure 3 shows the resistivity values as a function of pressure at 40 K (ρ@40K) in the insulating phases for $CuIr_2S_4$ (left axis) and $MgTi_2O_4$ (right axis), respectively. The values of ρ at 40 K for $CuIr_2S_4$ increase with pressure increasing, indicating the suppression of the metallic phase [28]. Nevertheless, those for $MgTi_2O_4$ decrease with pressure increasing, suggesting the enhancement of the metallic state. These results clearly demonstrate that the applied hydrostatic pressure has opposite effects on the transport behaviors of $CuIr_2S_4$ and $MgTi_2O_4$. For $CuIr_2S_4$, the pressure suppresses the metallic phase. Thus, the shrinkage of the metallic phase results in the increase of T_{MI} and the weakening of phase transition intensity. Contrarily, for $MgTi_2O_4$, the pressure enhances the metallic phase. Therefore, the expansion of the metallic phase leads to the decrease of T_{MI} and the enhancement of phase transition intensity.

Although the phase transitions in $CuIr_2S_4$ and $MgTi_2O_4$ are explained under a common framework of an orbitally-induced Peierls phase transition mechanism, our experimental results unambiguously demonstrate that the applied pressure has opposite effects on the transport behavior in these two systems. In fact, it has been noticed that there are some differences for the lattice distortions in these two systems. Experiments have demonstrated that the lattice structures change differently in these two systems when the phase transitions occur. In the low temperature insulating phase, the lattice constant $c/a = 1.033 > 1$ for $CuIr_2S_4$ [8], while that $c/a = 0.997 < 1$ for $MgTi_2O_4$ [13]. In other words, the c-axis is elongated in $CuIr_2S_4$ while it is compressed in $MgTi_2O_4$ when phase transitions occur. It is well known that the Peierls phase transition typically only occurs in one-dimensional

metallic chain due to the special one-dimensional band structure [29]. If a Peierls-like phase transition occurs in a three-dimensional material, a quasi-one-dimensional band structure should be expected in the system. For the spinel structure AB_2X_4, the crystal field Δ_{CF} generated by the BX_6 octahedron splits the d band into doublet e_g sub-band with higher energy and triplet t_{2g} sub-band with lower-energy, as shown in Fig. 4. In the present cases of $CuIr_2S_4$ and $MgTi_2O_4$, the partial filled t_{2g} sub-bands (including degenerate xy, yz, and zx) paly key roles in the phase transitions. However, only crystal field alone cannot give the desired quasi-one-dimensional band structure because the xy, yz, and zx levels of the t_{2g} sub-band are still degenerate. For the partial-filled triplet t_{2g} sub-band, the energy levels are further split through the elongation or compression of the lattice, which is known as the Jahn-Teller effect. The Jahn-Teller effect further splits and broadens the t_{2g} sub-band, which give rise to the required quasi-one-dimensional band structure [18]. The anisotropic orbital coupling is finally caused by the quasi-one-dimensional band originating from the Jahn-Teller effect, which leads to the orbitally-dependent hopping of electrons as encapsulated by the Kugel-Khomskii (KK) model [30–32]. In $CuIr_2S_4$, due to the elongation of lattice along the c-axis caused by the Jahn-Teller effect, yz and xz levels of Ir-t_{2g} sub-band are lowered. Considering $5d^5$ electronic configuration of Ir^{4+} ion, yz and xz levels are fully-filled and xy level is half-filled, as shown in the bottom panel of Fig. 4 (a). A strong orbital anisotropy is formed along the orbital lobe direction caused by the xy level, *i. e.* the xy (or [110]) direction as given in the middle panel of Fig. 4 (a). The anisotropic orbital coupling results in the orbitally-driven Peierls instability. In $MgTi_2O_4$, due to the compression of lattice along the c-axis caused by the Jahn-Teller effect, the xz and yz levels are lowered, as shown in the bottom panel of Fig. 4 (b). However, in view of $3d^1$ electronic configuration of Ti^{3+} ion, the degenerate yz and xz levels are occupied alternatively, resulting in the coupling along the alternative xz and yz directions (*i. e.* the chiral bonds along [001] direction), as shown in the middle panel of Fig. 4 (b). The coupling along two directions (xz and yz) in $MgTi_2O_4$ is more complex than that in $CuIr_2S_4$, however, still quasi-one-dimensional band structure is formed, as shown in the bottom panel of Fig. 4 (b).

The quasi-one-dimensional band structure also helps us to understand the opposite pressure effects in $CuIr_2S_4$ and $MgTi_2O_4$. The Jahn-Tell effect in low temperature phase implies that the phase transition would be directly influenced by the compression or expansion of the lattice. For $CuIr_2S_4$, applying pressure suppresses the elongation tendency along the

c-axis, resulting in the suppression of the metallic phase. The shrinkage of the metallic phase in $CuIr_2S_4$ results in the increase of T_{MI}, the weakening of the phase transition intensity, and the decrease of the resistivity values. Contrarily, for $MgTi_2O_4$, applying pressure improves the compressive tendency of c-axis, which causes the expansion of the metallic phase. The enhancement of the metallic phase in $MgTi_2O_4$ leads to the decrease of T_{MI}, the increase of the phase transition intensity, and the decrease of the resistivity values. This scenario is confirmed by the first-principle electronic structure calculations [26]. For revealing the influence of pressure effect more clearly, electronic structure calculations are performed using $P = 4$ GPa. Figures 5 (a) and (b) shows the total density of states (tDOS) of low-temperature phases under ambient and high pressure for $CuIr_2S_4$ and $MgTi_2O_4$, respectively. For $CuIr_2S_4$, part of the occupied states become unoccupied under pressure so that the tDOS around Fermi level decreases [see the inset of Fig. 5 (a)]. As the physical properties of a material are dominantly determined by the electronic properties around Fermi level, the reduction of the tDOS indicates that the system becomes more insulating under high pressure, which results in the increase of resistivity as observed in experiment. For $MgTi_2O_4$, part of the unoccupied states become occupied under pressure [see the inset of Fig. 5 (b)], which is opposite to that in $CuIr_2S_4$. Therefore, the system exhibits the enhancement of metallic tendency under pressure, which is consistent with the experimental observations. To better understand the pressure effects on the electronic properties, we plot the atomically-resolved DOS in the low temperature phase for $CuIr_2S_4$ and $MgTi_2O_4$ in Fig. 5 (c) and (d), respectively. From Fig. 5 (c), it can be seen that the decreased tDOS in $CuIr_2S_4$ is mainly due to the Ir ions. The S ions also have some contributions because of the hybridization between the S-3p and Ir-5d orbitals. From Fig. 5 (d), it is found that the increased tDOS is mainly due to the Ti ions, whereas the contribution from O or Mg is negligible, indicating the hybridization between Ti-3d and O-2p orbitals is rather weak. To summarize, the opposite behaviors under pressure in $CuIr_2S_4$ and $MgTi_2O_4$ are due to the different orbital ordering configurations (xy and xz/yz orbital ordering) caused by the elongated and compressed tetragonal distortions.

The orbitally-induced Peierls phase transition occurs in a three-dimensional network when a quasi-one-dimensional band structure emerges due to the interplay between the charge, spin, orbital, and lattice degreee of freedom. This kind of dimensionality reduction phenomena is quite rare. In additional to the typical $CuIr_2S_4$ and $MgTi_2O_4$ studied here, the

layered ruthenate $La_4Ru_2O_{10}$ and pyrochlore $Tl_2Ru_2O_7$ exhibit similar transitions [1, 2]. For $La_4Ru_2O_{10}$, it has been found that $b > a$ or c in low temperature phase, and spin-singlet formed by two $S = 1$ moments of Ru^{4+} ions [2, 33]. This suggests that $La_4Ru_2O_{10}$ should have similar pressure effect as that in $CuIr_2S_4$. The situation in $Tl_2Ru_2O_7$ is much more complicated [3]. It has been modeled as a one-dimensional zig-zag Haldane antiferromagnetic chain but not an orbitally-induced Peierls phase transition [3]. The $S = 1/2$ spin moments of Ru^{4+} ions do not form a spin-singlet but exhibit an antiferromagnetic order. The zig-zag ordering structure would lead to much more complicated pressure effect in $Tl_2Ru_2O_7$.

IV. CONCLUSION

In summary, we find that hydrostatic pressure have opposite effects on the orbitally-induced Peierls phase transitions in $CuIr_2S_4$ and $MgTi_2O_4$. For $CuIr_2S_4$, the transition temperature T_{MI} increases under applied pressure and the phase intensity gets weaker. In contrast, for $MgTi_2O_4$, T_{MI} decreases as the pressure increases and the transition intensity becomes stronger. These observations demonstrate that the applied pressure suppresses the metallic phase in $CuIr_2S_4$ while it enhances that in $MgTi_2O_4$. Based on the first-principle electronic structure calculations, we suggest that these differences originate from the different one-dimensional band-Jahn-Teller effects (xy, yz/xz) caused by different tetragonal lattice distortions.

V. ACKNOWLEDGEMENTS

This work was supported by the National Natural Science Foundation of China (Grant Nos. 11574322, U1332140, 11574315, 11504377, and 11574288), the State Key Project of Fundamental Research of China through Grant No. 2011CBA00111, and the Foundation for Users with Potential of Hefei Science Center (CAS) through Grant No. 2015HSC-UP001.

[1] P. Khalifah, R. Osborn. Huang, H. W. Zandbergen, R. Jin, Y. Liu, D. Mandrus, R. J. Cava, Science **297,** 2237 (2002).

[2] H. Wu, Z. Hu, T. Burnus, J. D. Denlinger, P. G. Khalifah, D. G. Mandrus, L. Y. Jang, H. H. Hsieh, A. Tanaka, K. S. Liang, J.W. Allen, R. J. Cava, D. I. Khomskii, L. H. Tjeng, Phys. Rev. Lett. **96,** 256402 (2006).

[3] S. Lee, J. G. Park, D. T. Adroja, D. Khomskii, S. Streltsov, K. A. Mcewen, H. Sakai, K. Yoshimura, V. I. Anisimov, D. Mori, R. Kanno, R. Ibberson, Nat. Mater. **5,** 471 (2006).

[4] M. Croft, V. Kiryukhin, Y. Horibe, S. W. Cheong, New J. Phys. **9,** 86 (2007).

[5] S. H. Baek, D. V. Efremov, J. M. Ok, J. S. Kim, J. Brink, B. Buchner, Nat. Mater. **14,** 210 (2015).

[6] P. G. Radealli, New J. Phys. **7,** 53 (2005).

[7] S. Nagata, T. Hagino, Y. Seki, T. Bitoh, Physica B **194-196,** 1077 (1994).

[8] T. Furubayashi, T. Matsumoto, T. Hagino, S. Nagata, J. Phys. Soc. Jpn. **63,** 3333 (1994).

[9] P. G. Radaelli, Y. Horibe, M. J. Gutmann, H. Ishibashi, C. H. Chen, R. M. Ibberson, Y. Koyama, Y. S. Hor, V. Kiryukhin, S. W. Cheong, Nature (London) **416,** 155 (2002).

[10] H. Ishibashi, T. Sakai, K. Nakahigashi, J. Magn. Magn. Mater. **226-230,** 233 (2001).

[11] M. Isobe and Y. Ueda, J. Phys. Soc. Jpn. **71,** 1848 (2002).

[12] H. D. Zhou and J. B. Goodenough, Phys. Rev. B **72,** 045118 (2005).

[13] M. Schmidt, W. Ratcliff, P. G. Radaelli, K. Refson, N. M. Harrison, S. W. Cheong, Phys. Rev. Lett. **92,** 056402 (2004).

[14] K. Takubo, S. Hirata, J. Y. Son, J. W. Quilty, T. Mizokawa, N. Matsumoto, S. Nagata, Phys. Rev. Lett. **95,** 246401 (2005).

[15] N. L. Wang, G. H. Cao, P. Zheng, G. Li, Z. Fang, T. Xiang, H. Kitazawa, T. Matsumoto, Phys. Rev. B **69,** 153104 (2004).

[16] J. Zhou, G. Li, J. L. Luo, Y. C. Ma, D. Wu, B. P. Zhu, Z. Tang, J. Shi, N. L. Wang, Phys. Rev. B **74,** 245102 (2006).

[17] In fact, there is competition between the spin-singlet state and a quadrupolar state in $CuIr_2S_4$. The former singlet state is a conventional one, adiabatically connected to the orbital Peierls state. The latter quadrupolar state is stabilized by the additional interaction, which consists of a linear combination of different total spin momenta along the spin quantization axis [see K. M. Kojima, R. Kadono, M. Miyazaki, M. Hiraishi, I. Yamauchi, A. Koda, Y. Tsuchiya, H. S. Suzuki, H. Kitazawa, Phys. Rev. Lett. **112,** 087203 (2014) and J. Nasu and Y. Motome, Phys. Rev. B **90,** 045102 (2014)].

[18] D. I. Khomskii and T. Mizokawa, Phys. Rev. Lett. **94,** 156402 (2005).

[19] M. Croft, W. Caliebe, H. Woo, T. Tyson, D. Sills, Y. S. Hor, S. W. Cheong, V. Kirykukhin, S. J. Oh,, Phys. Rev. B **67,** 201102 (2003).

[20] G. H. Cao, T. Naka, H. Kitazawa, M. Isobe, T. Matsumoto, Phys. Lett. A **307,** 166-171 (2003).

[21] G. H. Cao, T. Furubayashi, H. Suzuki, H. Kitazawa, T. Matsumoto, Y. Uwatoko, Phys. Rev. B **64,** 214514 (2001).

[22] G. Oomi, T. Kagayama, I. Yoshida, T. Hagina, S. Nagata, J. Magn. Magn. Mater. **140-144,** 157 (1995).

[23] L. Zhang, L. S. Ling, Z. Qu, C. J. Zhang, S. Tan, Y. H. Zhang, Europhys. Lett. **94,** 37003 (2011).

[24] Y. Y. Zhu, R. J. Wang, L. Wang, Y. Liu, R. Xiong, J. Shi, Appl. Magn. Reson. **46,** 505 (2015).

[25] A. P. Reyes, E. T. Ahrens, R. H. Heffner, P.C. Hammel, and J. D. Thompson, Rev. Sci. Instrum. **63,** 3120 (1992).

[26] See the supplementary material for the details of electronic structure calculation.

[27] L. Zhang, L. Ling, Z. Qu, W. Tong, S. Tan and Y. Zhang, Eru. Phys. J. B **77,** 83 (2010).

[28] A. B. Garg, V. Vijayakumar, B. K. Godwal, A. Choudhury, H. D. Hochheimer, Solid State Commun. **142,** 369-372 (2007).

[29] R. E. Peierls, *Quantum Therory of Solids*, Oxford Univ. Press (1955).

[30] K. I. Kugel and D. I. Khomskii, Sov. Phys. JETP **37,** 725 (1973).

[31] K. I. Kugel and D. I. Khomskii, Sov. Phys. Solid State **17,** 285 (1975).

[32] K. I. Kugel and D. I. Khomskii, Sov. Phys. Usp. **25,** 231 (1982).

[33] S. J. Moon, W. S. Choi, S. J. Kim, Y. S. Lee, P. G. Khalifah, D. Mandrus, T. W. Noh, Phys. Rev. Lett. **100,** 116404 (2008).

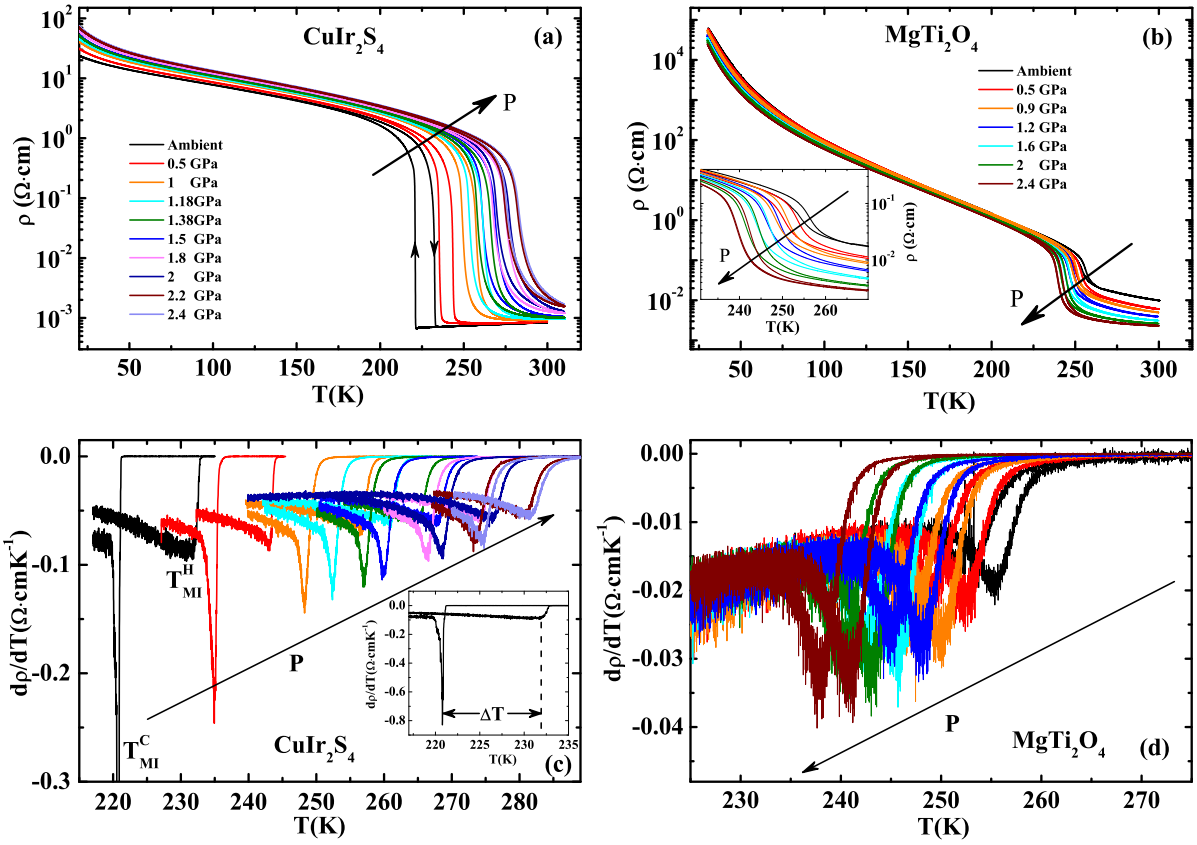

FIG. 1: (Color online) Temperature dependence of resistivity [$\rho(T)$] under different pressures for (a) $CuIr_2S_4$ and (b) $MgTi_2O_4$ [the inset of (b) shows the magnification of the phase transition for $MgTi_2O_4$]; temperature dependence of differential resistivity [$d\rho/dT(T)$] under different pressures for (c) $CuIr_2S_4$ and (d) $MgTi_2O_4$ [the inset of (c) shows the definition of ΔT].

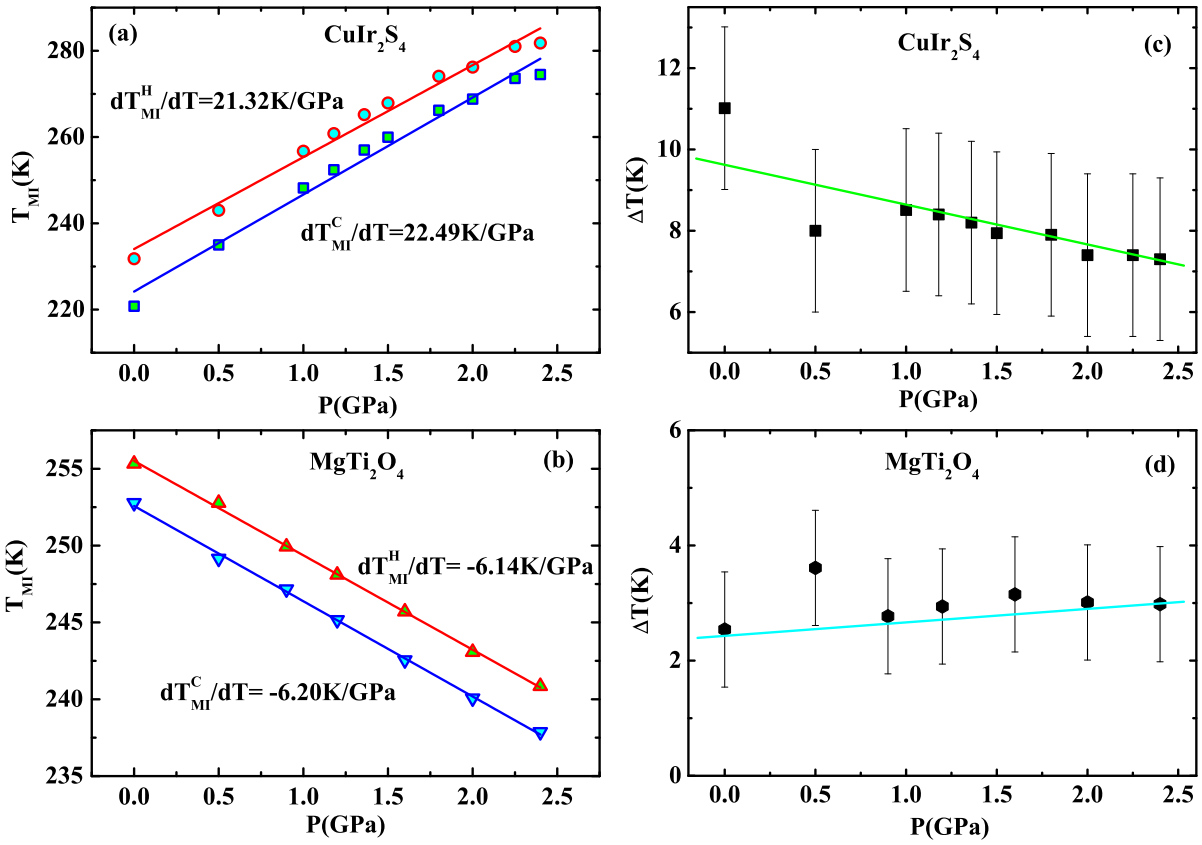

FIG. 2: (Color online) The transition temperature T_{MI} as a function of pressure for (a) $CuIr_2S_4$ and (b) $MgTi_2O_4$ (the solid lines are fitted); the pressure dependence of the phase transition width (ΔT) for (c) $CuIr_2S_4$ and (d) $MgTi_2O_4$ (the lines are guided on eye).

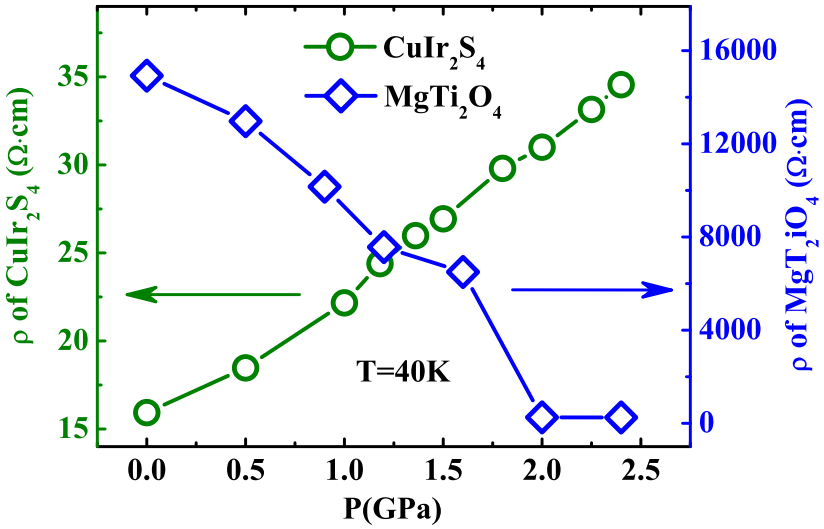

FIG. 3: (Color online) The resistivity of $CuIr_2S_4$ (right axis) and $MgTi_2O_4$ (left axis) at 40K (ρ@40K) as a function of pressure.

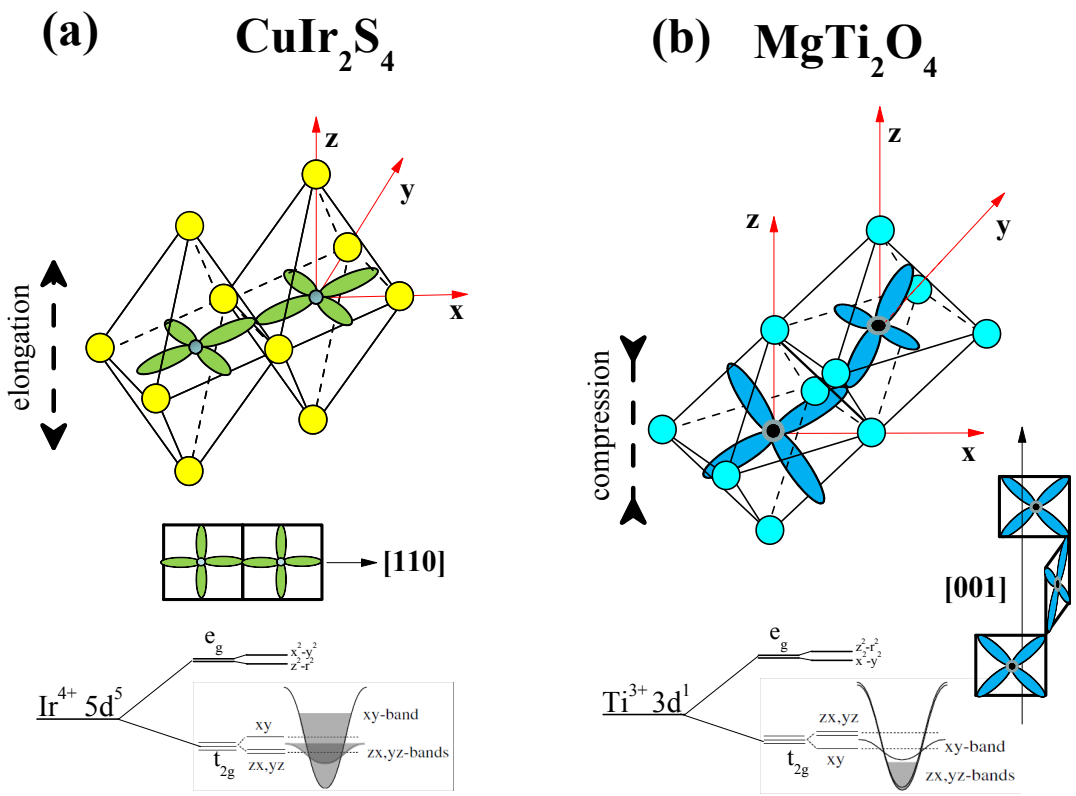

FIG. 4: (Color online) The diagrammatic sketch for the formation of the quasi-one-dimensional bands for (a) $CuIr_2S_4$ (left) and (b) $MgTi_2O_4$ (right) (the top panels illustrate the distorted octahedron of IrS_6 and TiO_6, the middle ones show the orbital overlap directions, and the bottom ones display the one-dimensional band structures).

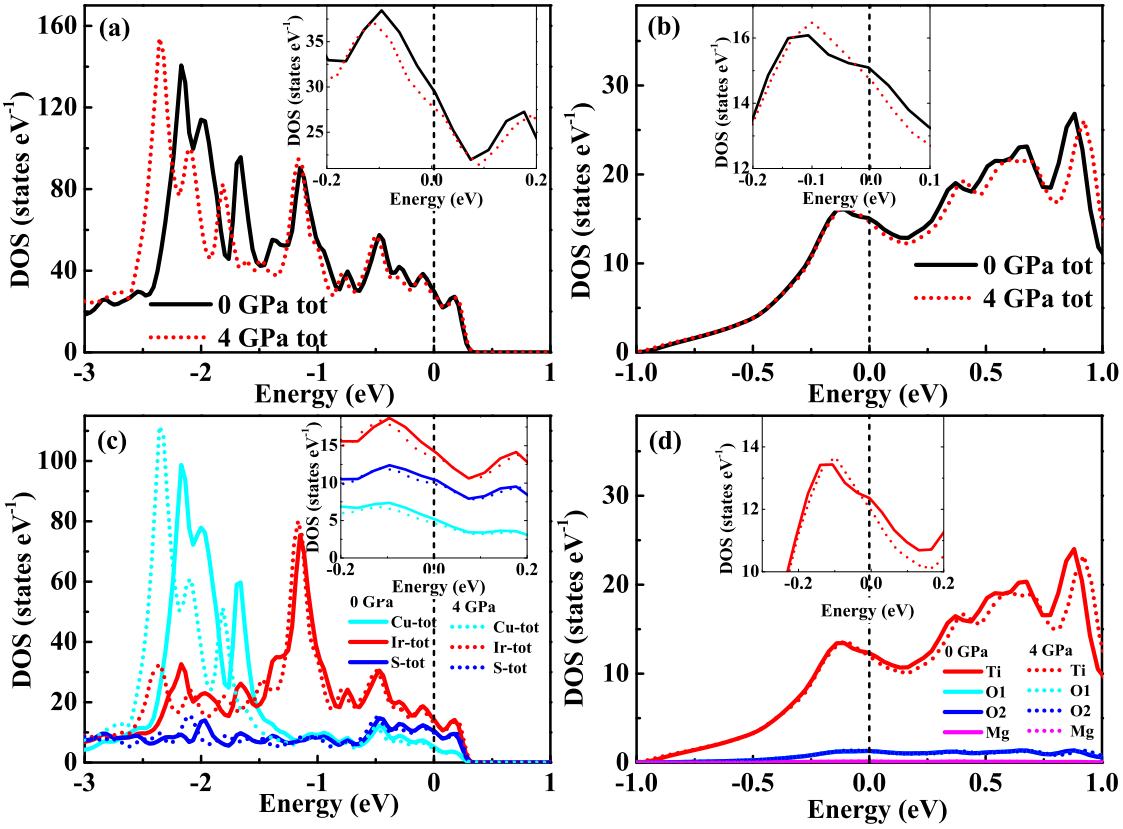

FIG. 5: (Color online) Total density of states (tDOS) in low temperature phases for (a) $CuIr_2S_4$ and (b) $MgTi_2O_4$; atomically-resolved DOS in low-temperature phase for (c) $CuIr_2S_4$ and (d) $MgTi_2O_4$ (the insets gives the magnification of the density of states around Fermi level).